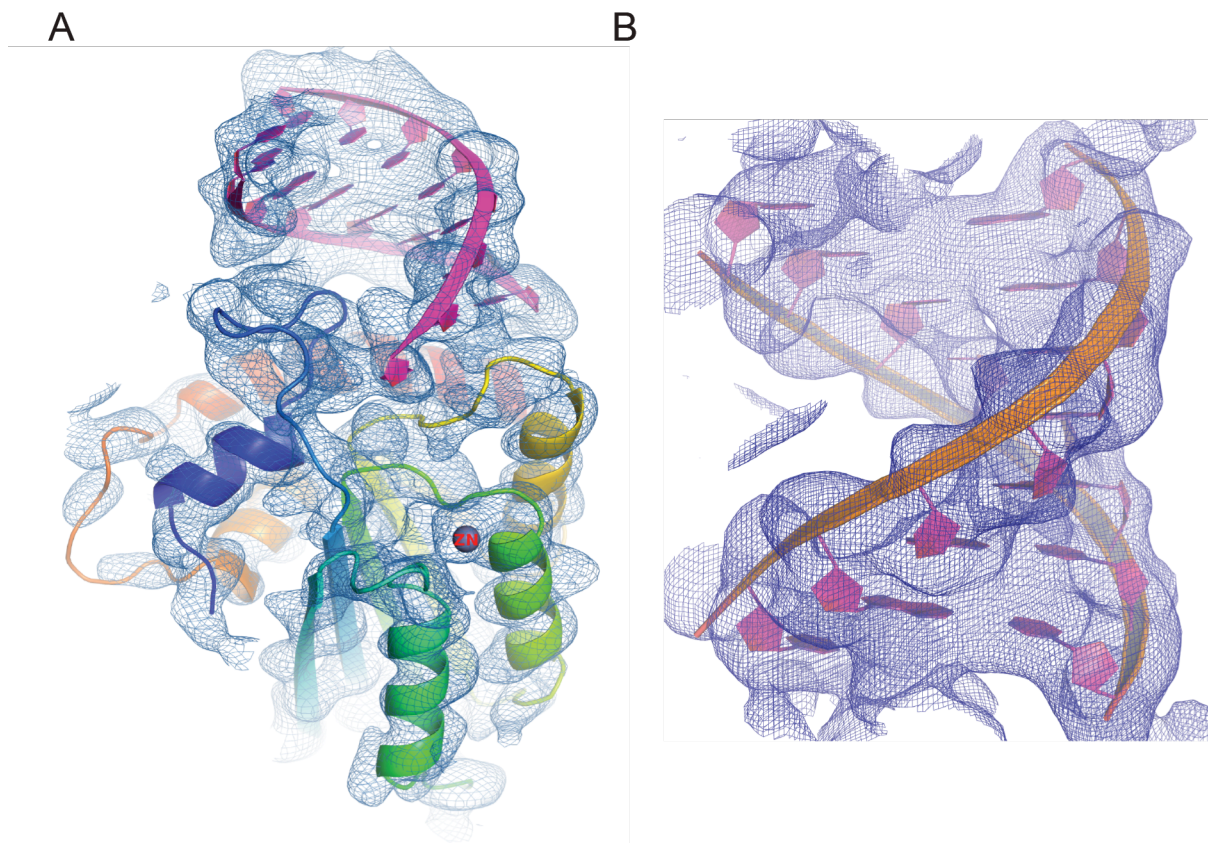


**Supplementary Materials** for:

**The Antiviral and Cancer Genomic DNA Deaminase APOBEC3H Is  
Regulated by an RNA-Mediated Dimerization Mechanism**

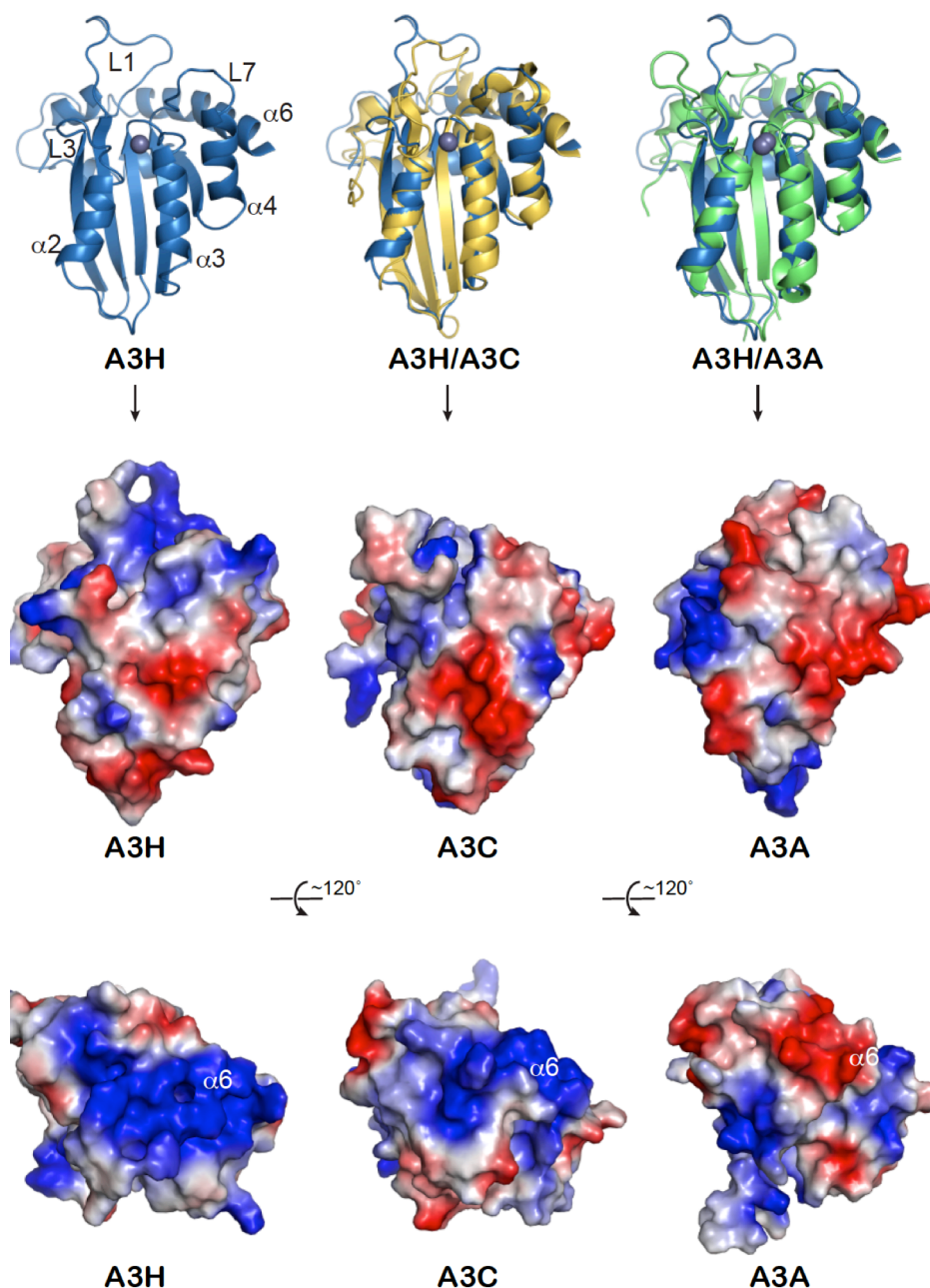
Nadine M. Shaban,<sup>1-4</sup> Ke Shi,<sup>1-3</sup> Kate V. Lauer,<sup>1-4</sup> Michael A. Carpenter,<sup>1-5</sup> Christopher  
M. Richards,<sup>1-4</sup> Michael W. Lopresti,<sup>1</sup> Daniel Salamango,<sup>1-4</sup> Jiayi Wang,<sup>1-4</sup> Surajit  
Banerjee,<sup>6</sup> William L. Brown,<sup>1-4</sup> Hideki Aihara,<sup>1-3</sup> and Reuben S. Harris<sup>1-5,7,\*</sup>

Supplementary Information: Figures S1, S2, and S3



**Supplementary Figure S1. Electron Density Map for APOBEC3H-Duplex RNA Crystal Structure**

(A and B) The experimental electron density map, obtained using SAD phasing method (see Methods) from zinc anomalous signal and contoured at  $1\sigma$  (blue and purple mesh), reveals an A-form RNA duplex in the A3H crystal structure. Density is clearly visible for double helical-RNA in an A-form structure. The final refined RNA has a C3'-*endo* conformation for each ribose sugar pucker. The final refined RNA also has an average X-displacement of  $-5.5 \text{ \AA}$ , an average rise between adjacent base pairs of  $2.86 \text{ \AA}$ , and an average twist angle between adjacent base pairs of  $29.3^\circ$ , respectively.

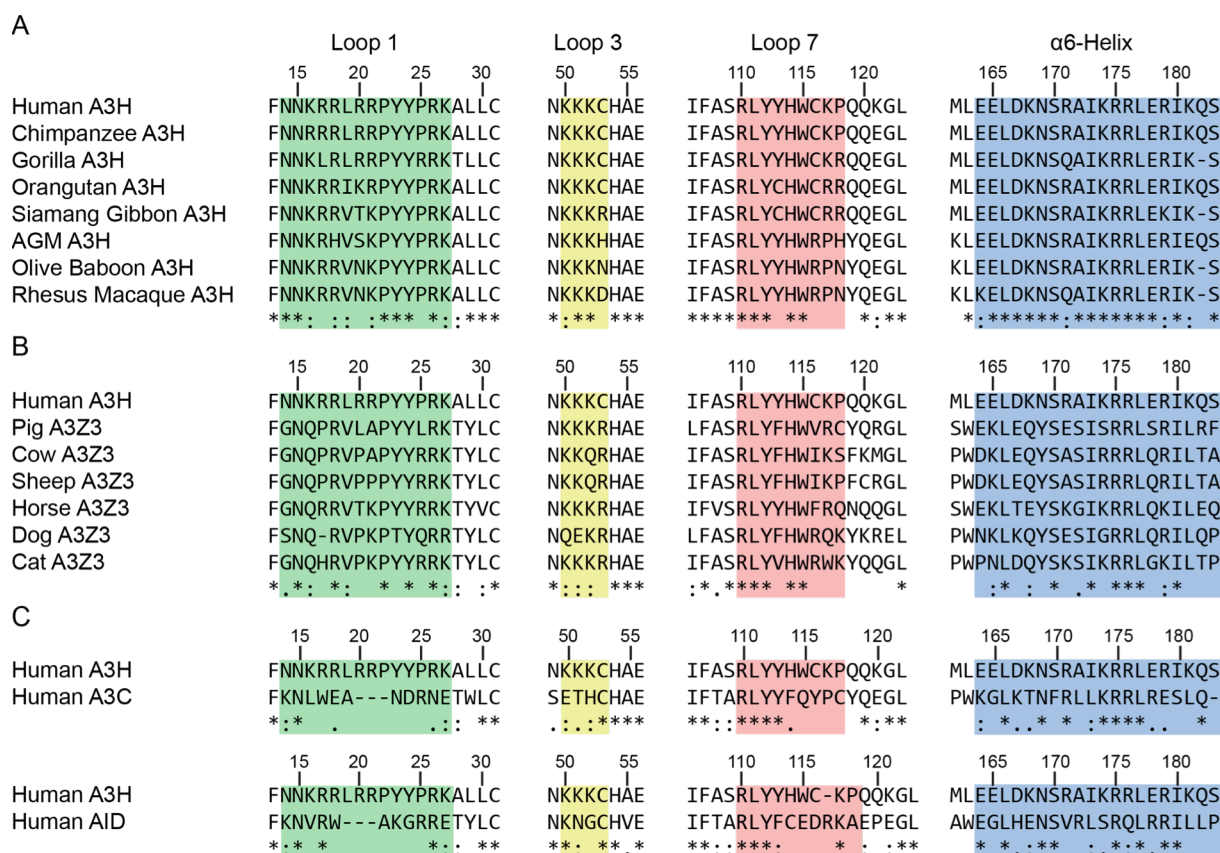


**Supplementary Figure S2. APOBEC3H Structure and Comparisons with Related APOBEC Family Members**

**Top row:** Ribbon schematic of an A3H monomer from the x-ray structure determined here in comparison by superposition with human A3A (pdb 5SWW) and human A3C (pdb 3V0W). Notable differences include a longer loop 1 in A3H, a shorter loop 3 in A3H, and an amino terminal 12-residue extension in A3A that has yet to resolve structurally.

**Middle row:** Electrostatic potential of A3H, A3A, and A3C in the same orientation as panel A, highlighting the conserved zinc-coordinating active site region.

**Bottom row:** 120 degree rotation of structures in the middle row, highlighting the RNA binding domain of A3H (patch 2) and a homologous basic patch in A3C. In contrast, A3A lacks an analogous positively charged surface region in the protein surface defined by the α6-helix.



### Supplementary Figure S3. APOBEC3H Conservation

(A) Clustal Omega alignment of human A3H and homologous primate A3H enzymes highlighting loop 1, loop 3, loop 7, and α6-helix regions. Numbers correspond to the 183 amino acid splice variant of human A3H haplotype II. GenBank accession numbers: Human A3H: NP\_861438.3; Chimpanzee A3H: NP\_001136078.1; Gorilla A3H: ACJ60858.1; Orangutan A3H: XP\_009232662.1; Siamang Gibbon A3H: ACJ60860.1; African Green Monkey (AGM) A3H: NP\_001332866.1; Olive Baboon A3H: NP\_001332865.1; Rhesus Macaque A3H: NP\_001332864.1.

(B) Clustal Omega alignment of human A3H and homologous mammalian A3Z3 enzymes. Format similar to panel A. GenBank accession numbers: Human A3H: NP\_861438.3; Pig A3Z3: ACH69768.1; Cow A3Z3: NP\_001333053.1; Sheep A3Z3: NP\_001154853.1; Horse A3Z3: NP\_001229380.1; Dog A3Z3: NP\_001333059.1; Cat A3Z3: NP\_001106181.2.

(C) Clustal Omega alignment of human A3H, A3C, and AID. Format similar to panel A. GenBank accession numbers: Human A3H: NP\_861438.3; human A3C: NP\_055323.2; human AID: NP\_065712.1.